Quaternary Science Reviews 178 (2017) 89–101

Contents lists available at ScienceDirect

Quaternary Science Reviews

journal homepage: www.elsevier.com/locate/quascirev

Cosmogenic evidence for limited local LGM glacial expansion, Denton Hills, Antarctica

Kurt Joy [a, b, *], David Fink [c], Bryan Storey [b], Gregory P. De Pascale [d], Mark Quigley [e], Toshiyuki Fujioka [c]

[a] University of Waikato, Private Bag 3105, Hamilton, New Zealand
[b] Gateway Antarctica, University of Canterbury, Private Bag 4800, Christchurch, New Zealand
[c] Institute for Environmental Research, ANSTO, PMB1, Menai 2234, Australia
[d] Department of Geology, University of Chile, Plaza Ercilla 803, Santiago, Chile
[e] School of Earth Sciences, The University of Melbourne. Parkville, Victoria 3010, Australia

ARTICLE INFO

Article history:
Received 10 April 2017
Received in revised form
19 October 2017
Accepted 1 November 2017
Available online 14 November 2017

Keywords:
Pleistocene
Holocene
LGM
Antarctica
Geomorphology
Glacial
Cosmogenic isotopes
Paleoclimatology

ABSTRACT

The geomorphology of the Denton Hills provides insight into the timing and magnitude of glacial retreats in a region of Antarctica isolated from the influence of the East Antarctic ice sheet. We present 26 Beryllium-10 surface exposure ages from a variety of glacial and lacustrine features in the Garwood and Miers valleys to document the glacial history of the area from 10 to 286 ka. Our data show that the cold-based Miers, Joyce and Garwood glaciers retreated little since their maximum positions at 37.2 ± 6.9 (1σ n = 4), 35.1 ± 1.5 (1σ, n = 3) and 35.6 ± 10.1 (1σ, n = 6) ka respectively. The similar timing of advance of all three glaciers and the lack of a significant glacial expansion during the global LGM suggests a local LGM for the Denton Hills between ca. 26 and 51 ka, with a mean age of 36.0 ± 7.5 (1σ, n = 13) ka.

A second cohort of exposure ages provides constraints to the behaviour of Glacial Lake Trowbridge that formerly occupied Miers Valley in the late Pleistocene. These data show active modification of the landscape from ~20 ka until the withdrawal of ice from the valley mouths, and deposition of Ross Sea Drift, at 10–14 ka.

© 2017 Elsevier Ltd. All rights reserved.

1. Introduction

Over the last few decades, terrestrial and marine geological records provided opportunities to study changes in ice sheet volume, global sea level, and paleo-climate during glacial and interglacial cycles (Zachos et al., 2001). The Antarctic ice sheets in particular were shown to respond significantly to warming and cooling climates, particularly during and since the Last Glacial Maximum (LGM) ~ 25–19 ka (Anderson et al., 2014; Larter et al., 2014; Mackintosh et al., 2014; Ó Cofaigh et al., 2014).

A 2014 special issue of Quaternary Science Reviews (Bentley et al., 2014) comprehensively synthesised thirty years of glaciological, geological and numerical modelling studies coupled with extensive field data to suggest that during warming and cooling periods, the East and West Antarctic ice sheets (EAIS & WAIS) respond in contrasting ways. During glacial episodes, ice at the grounding line-ice shelf contact advanced into shallow coastal basins, for example the grounded expansion of the WAIS into the Ross Embayment known as the Ross Ice Sheet (RIS; Greenwood et al., 2012; Hall et al., 2013), whilst interior continental regions experienced ice thinning (Ackert et al., 2013; Joy et al., 2014; Mackintosh et al., 2014). Conversely, during warmer interglacial climates in many sectors of Antarctica the opposite occurred with coastal ice margins retreating and thinning, while ice sheet interiors thickened (Ackert et al., 2007; Joy et al., 2014; Mukhopadhyay et al., 2012).

Although the overall understanding of Antarctic ice sheet response over the Quaternary has improved, particularly for cooler periods such as the LGM, relatively little is known about the specific and localised response of the numerous, largely coastal, valley glacier systems. The advance and retreat of such glaciers is likely to be more strongly controlled by local topography and catchment precipitation rather than the larger scale of regional Antarctic ice

* Corresponding author. University of Waikato, Private Bag 3105, Hamilton, New Zealand.
E-mail address: Kurt.Joy@waikato.ac.nz (K. Joy).

https://doi.org/10.1016/j.quascirev.2017.11.002
0277-3791/© 2017 Elsevier Ltd. All rights reserved.

sheet dynamics (Marchant et al., 1994; Swanger et al., 2017).

The complex mosaic of landscapes found throughout the ice-free areas of the Transantarctic Mountains provides an opportunity to investigate Quaternary Antarctic climate. Evidence from glacial (Denton and Marchant, 2000; Hall and Denton, 2000; Marchant et al., 1994) and paleo-lacustrine sediments (Hall et al., 2002, 2006) within the McMurdo Dry Valleys (MDV) suggest formation under a variety of climatic settings, with each valley having different glaciological, hydrological and topographic constraints. Therefore, understanding the role that geomorphic processes play in the formation of glacial valley deposits is key to their use as evidence of past Antarctic climate.

As geomorphological datasets from Antarctic mountain glaciers are rare, new datasets may provide important information about the evolution of glaciers and their relationship to climate. Additionally, the use of such datasets extends and augments other regional records, such as ice-cores and marine sediment cores, which albeit of far higher resolution than exposure age dating, pertain to atmospheric and marine systems.

Therefore, to investigate the relationship between landscape and glacial/interglacial climates prior to and following the LGM, we applied the technique of cosmogenic Beryllium-10 (^{10}Be) surface exposure dating (SED) to a variety of glacial landforms found in the Denton Hills within the MDV, an ice-free region on the western coast of McMurdo Sound (Fig. 1).

2. Regional setting

At the southern margin of the MDVs, the Denton Hills are a small ice-free and 'dry valley' region of polar desert (~200 km^2) isolated from the East Antarctic Ice Sheet to the west by the Royal Society Range and bordered to the east by the McMurdo Sound coast and Ross Ice Shelf (Fig. 1). The Denton Hills are dissected by east-trending coastal glacial valleys that drain into the western margin of the Ross Ice Shelf (RIS). The two largest valleys in the Denton Hills, the Miers and Garwood are each fed by a pair of glaciers, the Miers and Adams glaciers (Fig. 2A and B) and the Garwood and Joyce glaciers (Fig. 2C and D), respectively.

Sugden et al. (1995) suggested that, like the MDV, the valley systems of the Denton Hills were initially a product of Miocene glacial expansion. Their study showed that an advance of a warm-based EAIS into the Transantarctic Mountains that carved the region's U-shaped valleys and the subsequent overriding ice removed the majority of surficial regolith from higher elevations. However, the current valley morphology is the result of increased thickening of the RIS prior to and during the LGM, subsequent westward up-valley intrusion of grounded ice, pervasive thick permafrost conditions and development of post-LGM lacustrine and fluvial systems (Cox et al., 2012).

At the present-day, the Denton Hills are warmer than the northern Wright, Taylor and Victoria valleys and have one of the more temperate climates in Antarctica. Daily summer temperatures (December to February) ranging from −8.0 and 6.5 °C (Hawke and McConchie, 2001) with a mean of 0 °C. The area has prevailing anabatic easterly winds during summer and a noticeable absence of strong westerly katabatics that are commonly observed at other locations in the MDV (Hawke and McConchie, 2001). Cold-based glaciers within the Miers and Garwood Valleys are maintained due to low precipitation (~0.1 m a^{-1}), and limited residence time of summer snow that rapidly sublimates due to the low relative humidity (McConchie, 1989).

2.1. Glacial and lacustrine geomorphology of the Denton Hills

Miers Valley (78.1°S, 164.0°E, Fig. 1), one of the longest valleys in the Denton Hills, is ~15 km long, ~5 km wide with flanking ranges reaching elevations of >1000 masl (metres above sea level). The

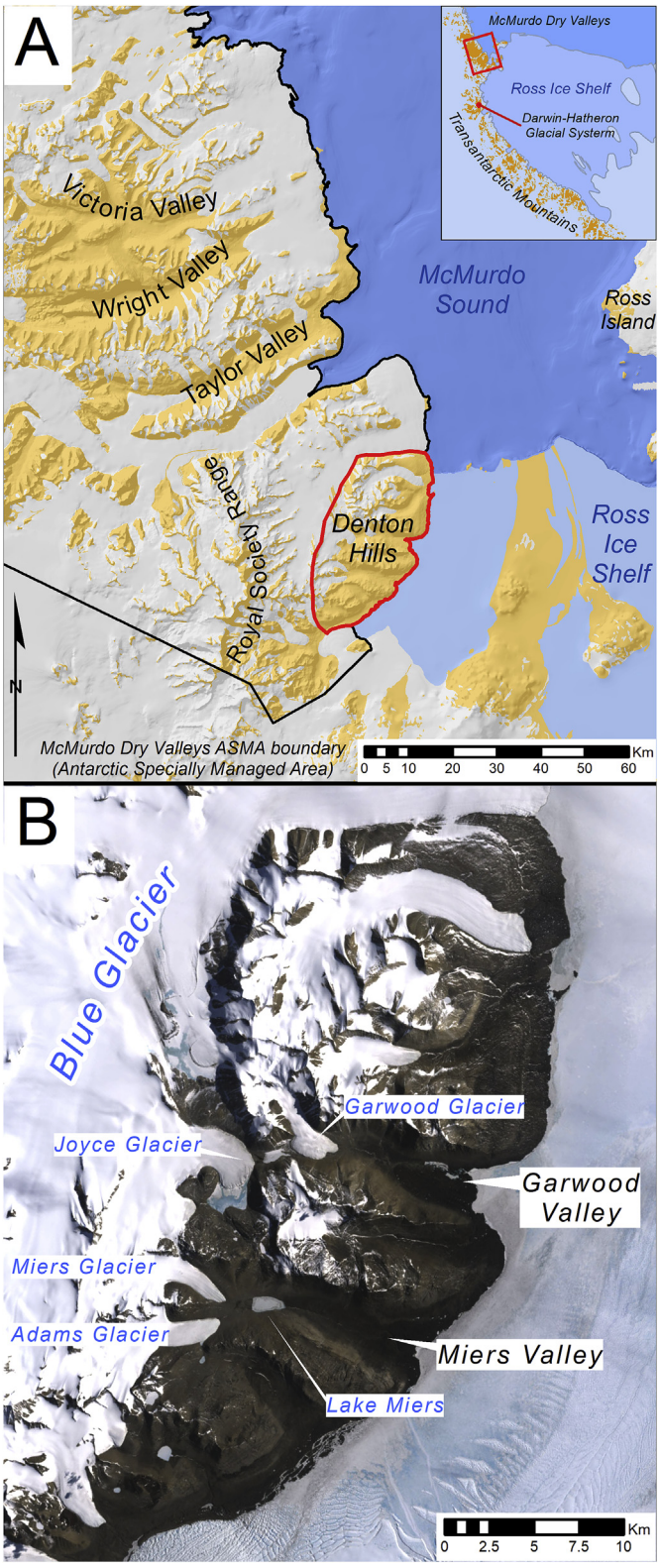

Fig. 1. McMurdo Sound, Antarctica. Area enclosed by the black line is the McMurdo Dry Valleys specially managed area, and by the red line is the Denton Hills. Also of note is another large ice-free area, the Darwin-Hatherton Glacial System, 200 km to the south. (For interpretation of the references to colour in this figure legend, the reader is referred to the web version of this article.)

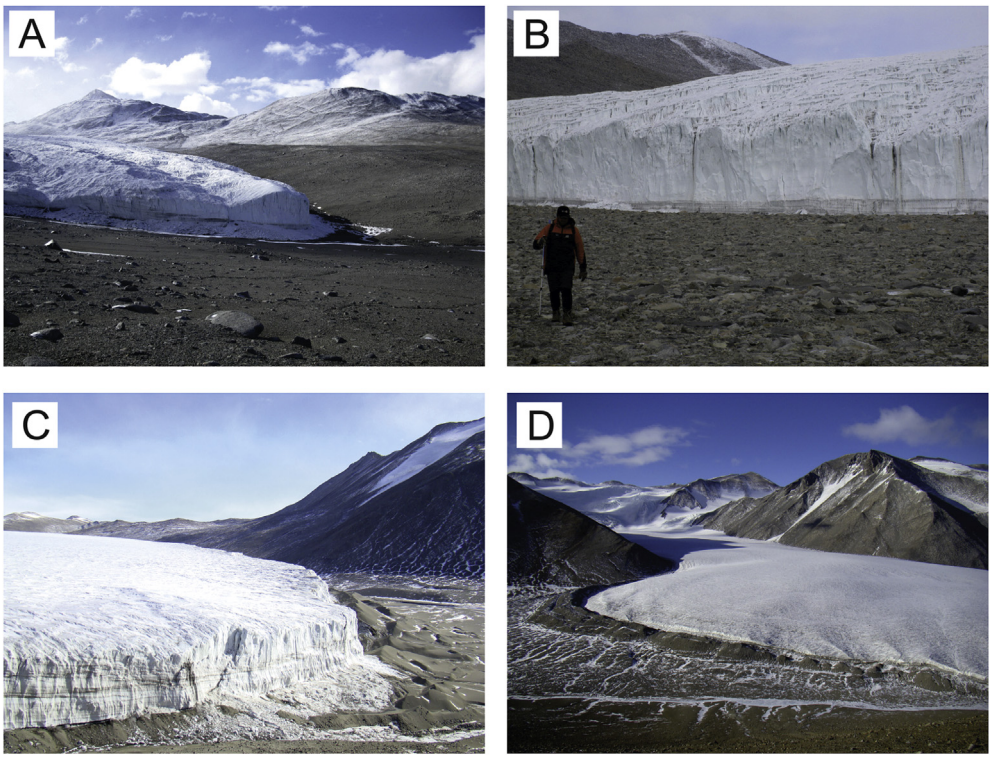

Fig. 2. Cold based glaciers located in the Denton Hills region. Glaciers display a typical cold-based morphology of sheer ice faces and thin lobes. (2A) Looking northward across the Miers Valley towards the Miers Glacier. (2B) The northern terminal ice face of the Adams Glacier. (2C) Looking west across the terminal push moraines at the margin of Joyce Glacier and Lake Colleen. (2D) The triple moraine at the terminal lobe of the Garwood Glacier.

valley contains two piedmont glaciers, the Miers and Adams, located at the valley head (Fig. 2A and B) that drain ice from the nearby Blue Glacier (77.9°S, 164.3°E). The Miers and Adams glaciers are morphologically similar to other cold-based Antarctic valley glaciers (Atkins, 2013) with narrow (<200 m wide) and thin (<100 m thick) central geometries that terminate on and drain into the valley floors. Their piedmont terminal ice lobes are characterised by vertical ice faces (~25 m high) with small ice aprons (2–4 m) that overlie a mix of modern and previously deposited glacial erratics and lacustrine material.

The main hydrological feature in Miers Valley, Lake Miers (Figs. 3 and 4), is similar to the other MDV lakes (e.g. Vida, Vanda & Hoare) and receives significant supra-glacial meltwater input from up-valley glaciers. With an area of 1.3 km^2, a depth of ~21 m and an ice cover of 3–5 m (Spigel and Priscu, 1998), the lake has one major outflow, the Miers River (Fig. 4), that runs through the Lower Miers valley eastward toward McMurdo Sound, and incises hummocky ice-cored moraines and a section of lacustrine evaporite deposits (Clayton-Greene et al., 1988).

The Garwood Valley (78.026°S, 164.144°E) (Fig. 1B), located 9 km to the north of the Miers Valley, has a similar morphology and size. Approximately 13 km long and 3.5 km wide with a typical glacially carved U-shaped morphology, the Garwood Valley is separated from its northern and southern neighbours by flanking bedrock ridges. As with the Miers Valley, the Garwood Valley has a pair of cold-based piedmont glaciers, the Joyce and Garwood (Fig. 2C and D), draining into the head of the valley. The larger of the two, Joyce Glacier, is fed from the Blue Glacier (Fig. 1) catchment and therefore shares a common ice source with the Miers and Adams glaciers. In contrast, the smaller Garwood Glacier, drains a ~10 km^2 local cirque in the mountains to the north of Garwood Valley and therefore is currently disconnected and isolated from the ice source feeding

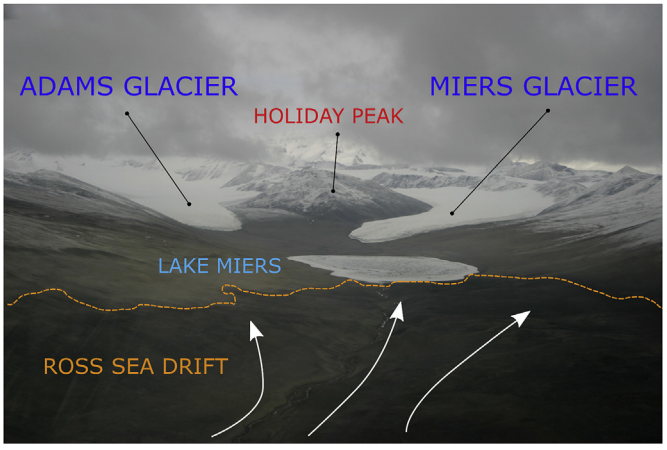

Fig. 3. Looking westward up the Miers Valley toward Lake Miers, Holiday Peak, the Adams and Miers (MG) glaciers. The dashed line demarcates the distinctive dark appearance of the Ross Sea Drift unit observed on the western floor of the Miers Valley. With proximity to the coast the drift becomes less subdued and the topographic influence of ice cored moraines becomes more pronounced. The direction of intruding LGM West Antarctic ice that deposited the material is shown by the arrows.

other glaciers in the area. The lobe of the Garwood Glacier bisects the upper valley region into a western and eastern section, with Lake Colleen (~800 m^2) occupying the western basin (Fig. 4A and D). Seasonal drainage of Buddha Lake (Fig. 4A) and supra-glacial meltwater from Joyce Glacier results in the formation of a large delta complex feeding into the western edge of Lake Colleen (Fig. 4D), that continues to drain eastward to the McMurdo coast via Garwood River (Levy et al., 2013).

Compared to the glacial landforms and deposits observed in

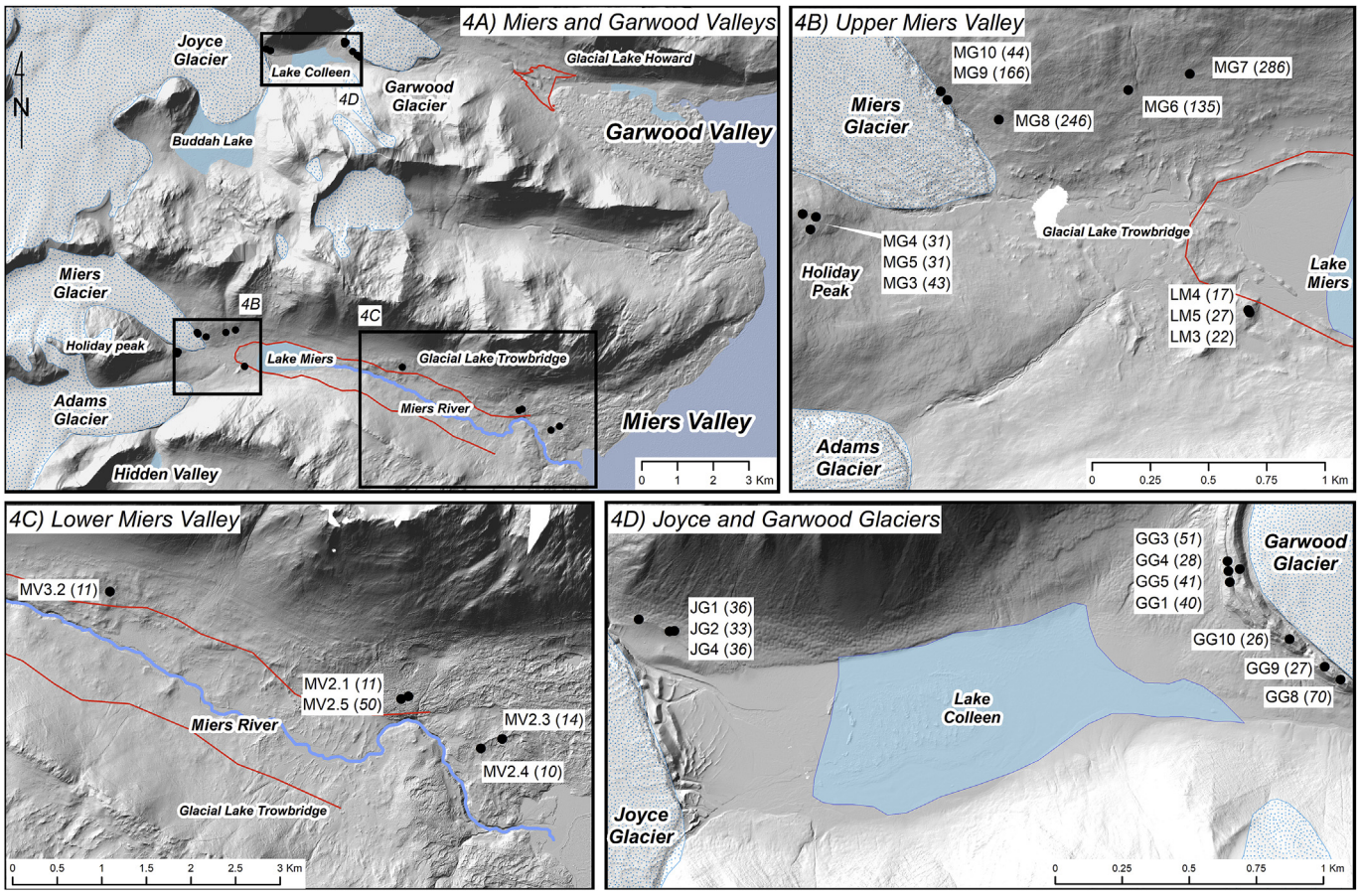

Fig. 4. (A), Sites selected for surface exposure dating within the Denton Hills. (B) Upper Miers Valley, including Lake Miers, Miers and Adams glaciers. (C) Lower Miers Valley, and (D) Garwood Valley, including the Joyce and Garwood glaciers. Samples marked by black dots have associated minimum central ^{10}Be exposure ages (bracketed; ka). The extents of Glacial Lake Trowbridge as inferred by Clayton-Green et al, (1988), and Glacial Lake Howard (Levy et al., 2013) are outlined by red lines. (For interpretation of the references to colour in this figure legend, the reader is referred to the web version of this article.)

Miers Valley, those of the Garwood Valley differ significantly. The Miers and Adams glaciers have limited constructional features associated with their advance and retreat, while in contrast, the Garwood and Joyce glaciers have a combination of both cold-based terminal-lateral boulder belts and distinct push moraines. This is most evident at the terminal face of Joyce Glacier where ice advancing over glacio-lacustrine sediments at the former margin of Lake Colleen, resulted in a complex of mound-like push moraines up to 30 m in height (Levy et al., 2013).

Garwood Glacier displays a very different style of ice marginal moraine from the cold-based boulder belts typically observed at stagnant ice margins (Atkins, 2013). In particular, the terminal moraine of Garwood Glacier reaches up to 40 m in height and is comprised of unsorted angular cobbles and boulders (rare examples up to ~4 m in diameter) that form three distinct terminal ridges at its western apron and merge to a single smaller ridge on the eastern side.

A distinctive and widespread feature present throughout the coastal sections of the MDVs is a glacial deposit known as the Ross Sea Drift (RSD). Characterised by dark coloured volcanic-rich hummocky moraines, the RSD intrudes westward from the McMurdo coast into the valleys of Denton Hills (Fig. 3), and is found at the mouths of the Miers and Garwood valleys. The extended distribution of RSD further northward along the McMurdo Sound coastline is significant as it has been used as one of the key lynchpins in reconstructing terminal positions, magnitudes and timing of LGM ice expansion within the Ross Embayment (Brook et al., 1995a,b; Denton and Marchant, 2000; Stuiver et al., 1981).

Across the Denton Hills, RSD is mapped as a younger (post-LGM) deposit overlying older sediment (Cox et al., 2012). Younger RSD deposits proximal to McMurdo coast are distinguished by ice cored moraines, abundant thermokarst, and areas of poorly developed patterned ground and desert pavements. In addition, an older RSD unit was described by Stuiver et al. (1981) as being related to an earlier and larger Pleistocene WAIS advance into the Ross Embayment. In the Garwood Valley, Levy et al. (2013) describe the “up-valley till” (i.e. older till) as having similar characteristics to younger RSD, but differentiated by an increase in clast weathering, with better-developed desert pavements and patterned ground. The presence of massive buried glacier ice underlying the complex of deltas suggests that the “down-valley till” (i.e. younger RSD) was emplaced directly on top of the older unit (Pollard et al., 2002; Levy et al., 2013).

Geochronological studies in the Denton Hills have primarily focused on the timing of LGM ice retreat, whilst some pre-LGM studies (Higgins et al., 2000) have been restricted by the maximum radiocarbon dating limit of ~50 ka. Prior to this work, age control for the RSD is predominantly from radiocarbon dating of organic material (e.g. algal mats) or carbonate sediments preserved at margins of former pro-glacial lakes within the MDVs (see Hall and Denton, 2000 for a review). As these pro-glacial lakes are understood to have formed against the ice margin of an expanded RIS,

the elevation contours and timing of paleo-lake shorelines may have been controlled by variations in thickness of damming ice (Hall et al., 2002; Hall et al., 2006). However, care is needed when equating algal radiocarbon ages to glacial retreat as two major assumptions need to be validated i.e. 1) that the increase in available water is a result of warming, and 2) that lake shoreline algal deposits are in-situ products and were not redeposited (Storey et al., 2010).

The existence of a large Pleistocene paleolake in Garwood Valley, named as Glacial Lake Howard (Fig. 4) is supported by the interpretation of ^{14}C ages from preserved deltas. Levy et al. (2013) suggest that an expanded RIS initially dammed Glacial Lake Howard ~26 ka cal BP and with successive ice thinning, the lake drained from ~7.3–5.5 ka cal BP as the grounding line retreated south and past the valley mouth. This is largely consistent with the suggested retreat history for the Ross Embayment (Anderson et al., 2014; Conway et al., 1999; Denton and Marchant, 2000; McKay et al., 2008, 2012) and with radiocarbon and $^{234}U/^{230}Th$ dates obtained from carbonate lacustrine deposits within the eastern basin from Miers Valley (Clayton-Greene et al., 1988) that suggest another large paleo-lake, Glacial Lake Trowbridge (Fig. 4) existed from 26 to 10 ka cal BP.

In addition to radiocarbon dating, a small number of studies have applied surface exposure dating (SED) on RSD deposits. Brook et al. (1995) measured terrestrial cosmogenic ^{3}He, ^{10}Be and ^{26}Al in both younger and older RSD distributed throughout the MDVs and the Denton Hills. A significant geological scatter was observed in younger RSD samples, presumably a result of an inheritance cosmogenic signal (Brook et al., 1995), with elevations from 250 to 400 masl giving ages ranging from 8 to ~106 ka with a mean of 33 ± 26 ka ($n = 19$). Older RSD deposits (370–550 masl) also display a very wide age scatter (104–572 ka), with a mean age of 253 ± 163 ka ($n = 7$). Of this second group, three samples directly originating from the older drift deposit in Miers and Garwood valleys (see Fig. 1 in Brook et al., 1995a,b) yielded ^{3}He exposure ages of 167 (Miers), 104 and 272 ka (Garwood), and a fourth sample from Blue Glacier gave an exposure age of 212 ka. The mean ages differentiate between an older and younger phase of RSD deposition. This concurs with field observations, weathering studies and geomorphic context (Stuiver et al., 1981) that suggest a Pleistocene age for the older RSD deposit.

3. Methodology

The use of SED has dramatically increased over the last few decades and consequently a better appreciation of the limitations in applying the technique in polar settings has emerged (Balco, 2011). In Antarctica, a number of factors can complicate interpretation of cosmogenic concentration as valid ages of the associated landform: 1) the preservation of older cold-based landforms which were overprinted by younger glacial advances (e.g. Atkins, 2013; Sugden et al., 1999), 2) the recycling of material with a pre-existing cosmogenic inventory (e.g. Storey et al., 2010; Joy et al., 2014), and 3) the susceptibility of deposited material to post-depositional modification (Applegate et al., 2010; Morgan et al., 2011; Putkonen et al., 2008).

Specifically, as a result of cold-based ice dynamics, coeval boulder clusters can be deposited over restricted areas such as at stagnant cold-based ice margins or alternatively distributed over large areas as sublimation drift (Atkins, 2013). Any combination of the above processes can lead to a situation where a complex geological scatter in exposure ages can be obtained from a single coeval landform (Fink and Smith, 2007; Hein et al., 2011; Storey et al., 2010; Strasky et al., 2009).

Detailed glacial mapping, identification of weathering limits and basal ice characteristics (cold-versus warm-based), and selecting the largest boulders or cobbles found on bedrock can often aid in reducing such outliers and geologic scatter in exposure age datasets. For example, combining perched cobble-bedrock pairs not only increases sample size but also provides a means to verify the passage of cold-based ice. However, when exposure ages are adversely impacted by such processes as described above, the analytical errors are usually too small to encompass the spread in the resultant age distribution and it becomes prudent to consider minimum or maximum age models. We suggest that the complexity of sampling at the margins of cold-based glaciers (Joy et al., 2014; Storey et al., 2010) warrants an initial interpretation based on selecting a minimum or maximum age model for a landform to assess chrono-stratigraphic relationships. A commonly adopted practice in other Antarctic studies is the 'mountain dipstick' mode where samples are typically collected over individual vertical transects on flanking mountain slopes with an objective to reconstruct past glacier surfaces and depth profiles (Mackintosh et al., 2007; Stone et al., 2003). In these studies, the youngest age at the highest elevation defines the most recent ice advance. However, given the presence of extensive drifts, limited elevation change between samples, and the prevalence of cold-based conditions, we consider that such an approach may not be suitable for our study.

3.1. Sample selection

Twenty-six samples were collected within the study area for SED. Table 1 summarises sample description, site data and local corrections to ^{10}Be production rates. The size of boulders targeted for surface exposure dating varied considerably from site to site (Table 1). Although boulders typically were of sub-metre size, a small number (i.e. MG6-10) were larger glacial erratics (1.5–3.5 m) emplaced on bedrock or subaerially exposed within glacial drift. The height of the upper boulder surface above the local ground tends to reduce issues that arise from snow shielding (though is a minor correction in this wind prone region) but more importantly, shielding due to exhumation of the boulder through glacial/moraine matrix following deposition and during the period of moraine stabilisation (see Heyman et al., 2016). Therefore, small clasts or cobbles perched on bedrock outcrops or large flat erratics are less likely to be impacted by sediment burial or reorientation during periods of moraine stabilisation. The remaining samples ranged in height above the host deposit from 0.1 m to 0.4 m.

Figures s1-s9 in supplementary section, provide representative photos of samples and locations.

3.1.1. Miers Glacier and Upper Miers Valley (MG)

At the head of Miers Valley, two groups of boulders were sampled from terminal and lateral moraines on the northern and southern glacial limits. The first group (MG3, 4 & 5, Fig. s1) was collected at an elevation slightly above the modern Miers Glacier margin. Here, a moraine wraps around the eastern ridge of Holiday Peak (Fig. 3) and conjoins with a similar feature at the similar elevation along the southern side. We conjecture the feature was constructed during the most recent ice advance and after a possible merging of the Miers and Adams glaciers. This moraine is comprised of generally small granitic boulders (<0.5 m) with little surficial relief. The second group of samples MG 8, 9 & 10 (Figs. s2 & s3), were collected from a similar setting on the northern flank of the glacier terminus. Here, a greater occurrence of very large erratics (>2 m) is observed and the site is ~70 m lower in elevation compared to that of the MG site described above.

Finally, samples MV 6 and 7 were taken from glacial drift deposits on slopes of the Upper Miers Valley (UMV, n = 2) at

Table 1
Sample and site description for Miers and Garwood valleys.

Sample ID	Location Latitude (S)	Location Longitude (E)	Altitude (masl)	Boulder Dimensions (LxWxH cm)	Thickness (cm)	Thickness Correction [a]	Topographic Correction
Miers-Adams Glaciers							
Upper Miers Valley							
MG6	78.0914	163.7717	238	400 × 350 x 350	1	0.991	0.998
MG7	78.0907	163.7831	237	350 × 300 x 250	6	0.948	0.998
Miers Glacier							
MG3	78.0971	163.7133	317	35 × 15 x 20	5	0.956	0.997
MG4	78.0966	163.7142	318	35 × 25 x 25	4	0.965	0.997
MG5	78.0965	163.7117	324	50 × 35 x 30	5	0.956	0.997
MG8	78.0927	163.7478	254	250 × 250 x 200	2	0.982	0.998
MG9	78.0920	163.7381	246	350 × 300 x 200	5	0.956	0.939
MG10	78.0917	163.7368	252	350 × 350 x 150	3	0.973	0.939
Lake Miers							
LM3	78.0997	163.7955	181	40 × 20 x 20	4	0.965	0.986
LM4	78.0998	163.7956	184	45 × 25 x 5	5	0.956	0.981
LM5	78.0997	163.7954	179	15 × 15 x 10	5	0.956	0.985
Lower Miers Valley							
MV2.3	78.0990	164.1015	27	15 × 10 x 3	3	0.973	0.996
MV2.1	78.1090	164.1308	72	20 × 12 x 20	3	0.973	0.995
MV2.5	78.1080	164.1343	75	18 × 15 x 4	4	0.965	0.996
MV2.4	78.1120	164.1808	40	15 × 15 x 5	3	0.973	0.996
MV3.2	78.0990	163.9871	120	15 × 15 x 5	5	0.956	0.996
Joyce-Garwood Glaciers							
Garwood Glacier							
GG1	78.0183	163.9045	409	90 × 50 x 40	3	0.973	0.996
GG3	78.0176	163.9040	412	20 × 15 x 20	5	0.956	0.997
GG4	78.0179	163.9042	400	50 × 45 x 20	5	0.956	0.996
GG5	78.0178	163.9060	420	15 × 15 x 15	5	0.956	0.991
GG8	78.0214	163.9228	388	60 × 40 x 40	5	0.956	0.990
GG9	78.0210	163.9202	391	70 × 40 x 50	4	0.965	0.992
GG10	78.0201	163.9144	389	70 × 30 x 15	5	0.956	0.994
Joyce Glacier							
JG1	78.0201	163.8097	390	40 × 30 x 40	5	0.956	0.992
JG2	78.0205	163.8155	387	30 × 25 x 10	4	0.965	0.993
JG4	78.0205	163.8147	390	50 × 30 x 25	5	0.956	0.993

[a] Based on an attenuation length of 150 g cm^2 and a rock density of 2.7 g cm^3.

elevations slightly lower and ~ 1 km down valley from those at the Miers glacier terminus (MG). Here a string of large boulders (>2 m) sit at a similar elevation above the valleys floor and may suggest glacial transport and deposition during a far older advance of the Miers Glacier.

3.1.2. Lake Miers (LM)

Samples collected at Lake Miers (LM, n = 3, Fig. s4) were from a prominent ridge, located ~1.4 km equidistant down valley from the modern terminus of Adams and Miers glaciers. As the upper surface of the ridge-like feature was relative free of high relief material, the three most pronounced clasts and boulders (0.05–0.20 m) were collected at an elevation of ~10 m above the current Lake Miers surface.

Given the up-valley curvature and concentric morphology of similar features to the north and west of Lake Miers, Clayton-Greene et al. (1988) suggested the ridges to be more representative of lake-level high stands as opposed to glacial construction. Therefore, these samples are likely related to the past expansion of Pleistocene Glacial Lake Trowbridge as mapped by Clayton-Greene et al. (1988).

3.1.3. Lower Miers Valley (MV)

In the lower (eastern) Miers Valley, a different methodology was required for those samples collected from the glacio-marine RSD material (MV, n = 5, Figs. s5 & s6). Material at this location was emplaced within drift deposits associated with the last retreat and/or sublimation of stranded ice. Given the relatively low topographic relief of these sites, sub-aerially exposed cobbles and boulders were collected directly from the exposed drift surface. This approach is well suited for both warm and cold-based glacial deposits draped across the landscape during periods of slow retreat or sublimation of stagnant ice, and has been used successfully at a number of ice-free Antarctic sites (Ackert and Kurz, 2004; Brook et al., 1993, 1995; Brown et al., 1991; Joy et al., 2014; Storey et al., 2010).

Five samples of RSD (MV) were preferentially collected east of Lake Miers, outside of the basin formally occupied by Glacial Lake Trowbridge and away from the reworked fluvial channel incised by the Miers River. Thus, samples were ensured of not being influenced by any post-depositional lacustrine or fluvial processes. The subdued topography and rare occurrences of large granitic boulders in this area, resulted in the collection of generally small boulders and cobbles emplaced in the desert pavement drift surface.

3.1.4. Garwood Glacier (GG)

At Garwood Glacier, seven samples (GG1, 3, 4, 5, 8, 9, 10; Figs. s7 and s8) were collected along the crest of a moraine complex that circumscribes the western and southern margin of the modern piedmont ice limits. Between 5 and 20 m in height, the moraines are comprised of unconsolidated angular granite and gneiss boulders (<1 m) and in-filled with a sand/silt matrix. These terminal moraine ridges are one of the most distinctive glacial features in the Denton Hills due to the uniqueness of its morphology and proximity to the present-day ice-margin. Moving along the ice front to the south-east towards the toe of the glacier this moraine complex appears to merge into a single moraine of ~500 m in length.

Table 2
AMS results and zero erosion exposure ages for the Miers and Garwood valleys.

Sample ID	$^{10}Be/^{9}Be$ ratio [a] (x 10^{-15})	Quartz mass (g)	^{9}Be carrier mass [b] (mg)	^{10}Be Concentration [c] (atom g^{-1} x 10^{3})	^{10}Be production rate [d] (atm/g/yr)	Minimum ^{10}Be exposure age [d,e] (ka)
Miers-Adams Glaciers						
Upper Miers Valley						
MG6	3108 ± 77 (2.5%)	85.08	0.3370	824 ± 27	6.49	135.0 ± 12.8 (4.6)
MG7	4570 ± 180 (2%)	65.19	0.3430	1606 ± 73	6.22	285.6 ± 29.7 (13.9)
Miers Glacier						
MG3	669.0 ± 18.3 (2.7%)	80.10	0.4974	277.6 ± 9.8	6.79	42.6 ± 4.0 (1.5)
MG4	615.2 ± 31.2 (5.1%)	80.46	0.4038	206.3 ± 11.4	6.85	31.2 ± 3.2 (1.7)
MG5	509.1 ± 16.8 (3.3%)	79.08	0.4777	205.5 ± 8.2	6.84	31.2 ± 3.0 (1.3)
MG8	5398 ± 37 (0.7%)	84.58	0.3450	1473 ± 34	*6.54*	*245.6 ± 23.1 (6.0)*
MG9	3129.2 ± 30.6 (1%)	89.62	0.3960	924.0 ± 23.2	*5.96*	*166.1 ± 15.4 (4.3)*
MG10	433.2 ± 14.3 (3.3%)	38.16	0.3370	256.0 ± 10.1	6.09	43.7 ± 4.2 (1.7)
Lake Miers						
LM3	472.8 ± 10.3 (2.2%)	100.62	0.4080	128.1 ± 4.0	5.90	22.4 ± 2.1 (0.7)
LM4	237.2 ± 8.6 (3.6%)	80.26	0.4727	93.4 ± 4.0	5.84	16.5 ± 1.6 (0.7)
LM5	537.0 ± 10.3 (1.9%)	99.99	0.4185	150.2 ± 4.4	5.83	26.6 ± 2.4 (0.8)
Lower Miers Valley						
MV2.3	133.4 ± 4.1 (3.1%)	71.45	0.5604	69.9 ± 2.7	5.10	14.1 ± 1.3 (*0.5*)
MV2.1	100.4 ± 4.4 (4.4%)	71.39	0.6178	58.0 ± 2.9	5.53	11.2 ± 1.1 (*0.6*)
MV2.5	466.2 ± 12.6 (2.7%)	76.24	0.6274	256.4 ± 9.0	*5.33*	*50.0 ± 4.7 (1.8)*
MV2.4	86.5 ± 3.7 (4.3%)	69.93	0.6287	52.0 ± 2.5	5.17	10.3 ± 1.0 (0.5)
MV3.2	22.6 ± 1.4 (6.2%)	10.48	0.3909	56.3 ± 3.7	5.54	10.5 ± 1.1 (0.7)
Joyce-Garwood Glaciers						
Garwood Glacier						
GG1	1133.7 ± 11.4 (1.1%)	101.49	0.3930	293.4 ± 7.2	7.55	40.4 ± 3.6 (1.0)
GG3	1302.6 ± 12 (0.9%)	98.23	0.4120	365.1 ± 8.8	7.46	51.0 ± 4.6 (1.2)
GG4	292.7 ± 10.4 (3.6%)	47.46	0.4891	201.6 ± 8.5	7.36	28.4 ± 2.7 (1.2)
GG5	783.3 ± 17.2 (2.2%)	80.58	0.4525	294.0 ± 9.2	7.47	40.9 ± 3.8 (1.3)
GG8	1768.4 ± 20.2 (1.1%)	102.05	0.4176	483.6 ± 12.1	*7.23*	*70.1 ± 6.3 (1.8)*
GG9	483.8 ± 15.1 (3.1%)	79.40	0.4744	193.2 ± 7.4	7.33	27.3 ± 2.6 (1.1)
GG10	505.6 ± 18 (3.6%)	80.19	0.4240	178.7 ± 7.5	7.27	25.5 ± 2.4 (1.1)
Joyce Glacier						
JG1	371.7 ± 10.5 (2.8%)	46.50	0.4736	253.0 ± 9.1	7.26	36.2 ± 3.4 (1.3)
JG2	735.4 ± 12.9 (1.8%)	80.42	0.3840	234.7 ± 6.7	7.31	33.4 ± 3.0 (1.0)
JG4	430.9 ± 16.1 (3.7%)	54.66	0.4750	250.2 ± 10.9	7.27	35.7 ± 3.5 (1.6)

[a] Measured against NIST SRM-4325 with a nominal value of 27900 × 10^{-15}. AMS ratio is the weighted mean of repeat measurements. Error is the larger of total statistical error or weighted error in mean. All ratios corrected for chemistry processing blanks with $^{10}Be/^{9}Be = 4.2 \pm 2.9 \times 10^{-15}$ (n = 4, 2 targets).
[b] ^{9}Be spike from solution of beryl crystal with 1385 ± 1% μg ^{9}Be/g solution.
[c] Additional 2% error added in quadrature based on reproducibility of AMS standard measurements for ^{10}Be and 1% error in ^{9}Be spike solution concentration.
[d] Production rates calculated using Cronus version 2.3 Lal/Stone scaling scheme (https://hess.ess.washington.edu/math/al_be_v23/al_be_multiple_v23.php).
[e] Bracketed values are internal (analytical) errors.

3.1.5. Joyce Glacier (JG)

Approximately 200 m north of Joyce Glacier, a number of small lateral moraines are perched above the Garwood Valley floor. The uppermost moraine (~390 masl) runs for approximately 500 m along the northern valley with an upper surface slightly dipping to the east (<5°). The moraine is composed of relatively consolidated material with medium sized boulders partially buried and protruding from the upper surface. This moraine is comprised of generally small granitic boulders (<0.5 m) with little surficial relief.

Three granitic boulders, JG1, JG2 and JG4 (Fig. s9) were collected from the inner crest to minimise the possibility of sampling material originally sourced from the valley wall.

3.2. Sample preparation, AMS measurement and age calculation

Sample preparation was carried out at the University of Canterbury's cosmogenic preparation facility based on procedures given in Child et al. (2000), and Mifsud et al. (2012). The sampled lithologies are granitoids from the Granite Harbour Intrusive Complex (Cox et al., 2012) with a recoverable cleaned quartz percentage in the 212–500 μm fraction of approximately 40–45% of the total sampled mass. Following Beryllium Oxide (BeO) extraction, $^{10}Be/^{9}Be$ ratios were measured on the tandem accelerator mass spectrometer (AMS) at the ANSTO ANTARES facility in Sydney, Australia (Fink and Smith, 2007) with ^{10}Be normalised against the NIST-4325 standard reference material ($^{10}Be/^{9}Be$ ratio of 27900 × 10^{-15}). A full discussion on background and AMS corrections can be found in Storey et al. (2010).

Measured ^{10}Be concentrations were converted to exposure ages using the CRONUS-earth exposure age calculator (version 2.3, Balco et al., 2008), and Stone et al. (2003) scaling methods. This online calculator (https://hess.ess.washington.edu/) uses the sea-level high latitude calibration spallation production rate of 4.49 at g^{-1} a^{-1} from Stone et al. (2003), which has been renormalised according to the re-adjustment of AMS $^{10}Be/^{9}Be$ standard reference materials (Nishiizumi et al., 2007). Although the calculator provides ages for other production rate scaling schemes (Desilets et al., 2006; Dunai, 2000; Lifton et al., 2008), to maintain consistency with the majority of other Antarctic exposure age studies (Ackert et al., 2013; Joy et al., 2014; Lilly et al., 2010; White et al., 2011; Yamane et al., 2011), site specific ^{10}Be production rates were calculated based on the time-independent scaling schemes of Stone et al. (2003) and the adjusted production rates in table 6 of Balco et al. (2008).

Exposure ages were calculated using a^{10}Be decay constant of 4.99 × 10^{-7} a^{-1}, based on the half-life value of 1.387 ± 0.012 Ma (Korschinek et al., 2010).

All quoted age errors are analytical errors only and do not

include the estimated 9% production rate uncertainty. To maintain consistency with other Antarctic cosmogenic studies (Lilly et al., 2010; Hein et al., 2011; White et al., 1011; Ackert et al., 2013; Suganuma et al., 2014; Kaplan et al., 2017), our exposure ages employ a zero-erosion rate. Therefore, all calculated exposure ages should be considered modelled minimum, unless prior exposure is suspected. For illustrative purposes, using an erosion rate of 0.5 mm/ka (a value considered high for Antarctic conditions) would increase young ages (<50 ka) by 13%–15% and older ages (~100–200 ka) by 20%–28%.

4. Results

Our dataset of 26 ^{10}Be surface exposure ages (Fig. 4) have a zero-erosion age range of 10 ka to 286 ka and cover altitudes of 27–420 masl (Table 1). Of the 22 acceptable ages (four are outliers) three individual ages are Early Holocene at 10–11 ka, two ages lie within Termination-1at 14 and 17 ka, and 15 ages are spread between 23 and 51 ka spanning Marine Isotope Stage (MIS) 2–4 and the remaining two pre-date the last glacial cycle and range from 135 to 286 ka.

When referred to our defined individual landforms and their stratigraphic relationship, a total of four samples, MV2.5 (50 ka), GG8 (70 ka), MG8 (246 ka) and MG9 (166 ka), can be classed as outliers being three to four times larger (i.e. older) than mean ages from the same landform as estimated from the remaining population. We plot in Fig. 5 exposure ages versus elevation above sea-level. Within each location, ages show an internal consistency (i.e. well clustered), however the apparent overall age-elevation linear correlation should not be used to infer an ice thinning rate over time. Although the maximum elevation difference is large (i.e. ~400 m), each set of samples comes from a distinct sub-group of the population, spread over three different valley glaciers, and as such are representative of different geomorphological settings and processes, hence precluding a 'dipstick' approach to quantify a regional ice surface lowering rate.

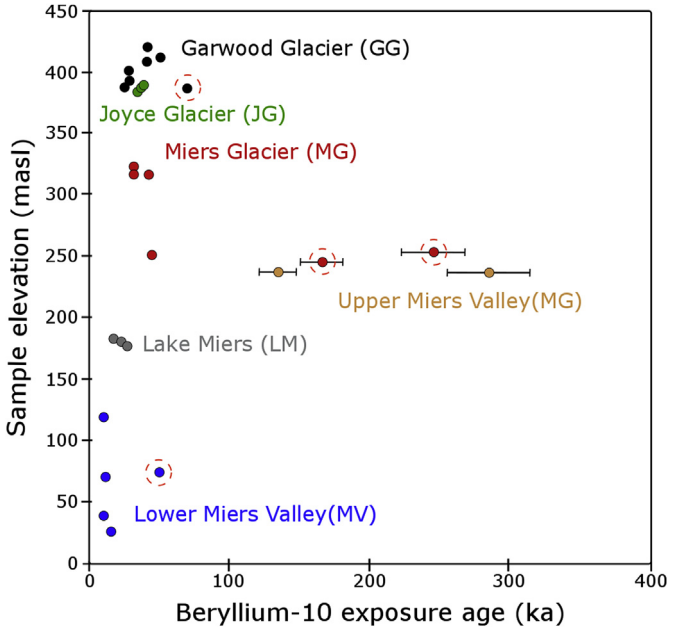

Fig. 5. Age-Elevation relationship plots for the Denton Hill SED samples. Samples collected from various discrete landforms cluster in groups (coloured dots) with the four samples (GG8, MG8, MG9 and MV2.5) considered outliers marked with red dotted circles. 2 sigma age errors are approximately the same size as the marker, so therefore have been omitted for clarity. (For interpretation of the references to colour in this figure legend, the reader is referred to the web version of this article.)

4.1. Miers Valley

At the Miers Glacier (Fig. 4B), six granitic boulders were dated in two groups at moraines near the glacier terminus. The first group (MG3, 4 & 5) has ^{10}Be ages of, 42.6 ± 4.0, 31.2 ± 3.2 and 31.2 ± 3.0 ka respectively, while within the second group (MG8, 9 & 10), only one (MG10) of the three boulders gives an exposure age (43.7 ± 4.2 ka) within that of MG 3,4 and 5. Therefore, a mean age of 37.2 ± 6.9 ka (1σ, n = 4) is assigned. The ages of the older two, MG9 and MG8, are among the oldest in our dataset, 166.1 ± 15.4 ka and 245.6 ± 23.1 ka, respectively, and are in stark contrast to the far younger ages (i.e. 31–44 ka).

Samples MG6 and 7, in the Upper Miers Valley and situated about 1 km due east from the modern glacier edge (Fig. 4B), gave ^{10}Be ages of 135.0 ± 12.8 and 285.6 ± 29.7 ka. These ages are anomalously old when compared to the younger ages in our dataset.

In the lower Miers Valley (Fig. 4C), samples MV2.1, MV2.3, MV2.4, and MV3.2 collected from the RSD, yield exposure ages of 11.2 ± 1.1, 14.1 ± 1.3, 10.3 ± 1.0 and 10.5 ± 1.1 ka respectively (Fig. 4); giving a mean age of 11.5 ± 1.8 ka (1σ, n =). Given the weathered and rounded appearance of MV2.5 (50 ka, the oldest sample) we conclude that it should considered an outlier and likely has some degree of prior exposure.

At Lake Miers (Fig. 4C), samples LM3, LM4 and LM5 have ^{10}Be exposure ages of 22.4 ± 2.1, 16.5 ± 1.6 and 26.6 ± 2.4 ka, with a mean age of 21.8 ± 5.1 (1σ, n = 3) ka. The lacustrine context most likely explains the very large spread of ages resulting from complex exhumation histories. This would preclude any glacially-related conclusion to be drawn from these ages other than a suggestion of LGM provenance.

4.2. Garwood Valley

At the Joyce Glacier (Fig. 4D), ^{10}Be ages from boulders JG1, JG2 and JG4, were 36.2 ± 3.4, 33.4 ± 3.0 and 35.7 ± 3.5 ka, with a mean age of 35.1 ± 1.5 (1σ, n = 3).

Eight samples in our dataset originated from the Garwood Glacier moraine complex. The first cluster, containing samples GG1, GG3, GG4 and GG5, were collected from a single locality across the western side of the moraine and have exposure ages of 40.4 ± 3.6, 51.0 ± 4.6, 28.4 ± 2.7 and 40.9 ± 3.8 ka respectively (Fig. 4D). A second set of three boulders (GG8, GG9 & GG10) were collected ~500 m to the east on the (convergent) single moraine at the ice terminus and gave ages of 70.1 ± 6.3, 27.3 ± 2.6 and 25.5 ± 2.4 ka, respectively (Fig. 4D). Given that age for GG-8 is ~2–3 times older than the other sample ages along the moraine ridges, we suggest that it can be considered as an outlier. The remaining six samples range from 26 to 51 ka with an overall population mean age of 35.6 ± 10.1 (1σ, n = 6) ka. This age distribution could be interpreted as a ca. 26–40 ka moraine with varying amounts of inheritance (minimum age model) that accounts for older ages, or an older moraine that contains some boulders with complex burial-exposure histories; we are unable to distinguish between these end-member scenarios and thus present age ranges and means herein.

5. Discussion

5.1. Interpretation of exposure ages

5.1.1. Ross Sea Drift and Glacial Lake Trowbridge

A Ross Sea Drift ^{10}Be mean age of 11.5 ± 1.8 ka is consistent with the presence of a grounded RIS damming the coastal mouths of the Denton Hills prior to 12 ka (Anderson et al., 2014; Hall et al., 2013). As the RSD samples are spread over an elevation range of ~90 m (27–120 masl) and have consistent ages they suggest that rapid thinning of at least 120 m ice thickness may have occurred, commencing at about 14 ka up to ~10 ka by which time the coastal parts of Miers Valley would have been basically ice-free (Fig. 6). Additionally, the tight clustering of ages, spread over ~20 km^2 may indicate that the RSD was deposited by a combination of overall ice surface lowering (i.e. ablation and sublimation down-wasting) and rapid down-valley retreat (Fig. 6). These interpretations are consistent with the timing of RIS retreat in the Ross Embayment: sediment cores from McMurdo Sound show grounded ice started to unground and retreat southward at ~10 ka transitioning to a floating ice shelf by ~8.8 ka ^{14}C cal BP (McKay et al., 2016). Our age data are consistent with the "swinging gate" model (Conway et al., 1999; Hall et al., 2013) of Ross Embayment deglaciation which suggests the RIS in McMurdo Sound was still at its maximum thickness and extent by as late as 13 ka, when thinning began.

Our conceptual model for RSD deposition in the Miers Valley is that as the grounding line retreated southward along the McMurdo coast, ice which originally filled the Denton Hill valleys thinned and/or retreated via ablation and sublimation. The reduction of ice volume would have then concentrated the entrained RSD material and eventually formed the extensive RSD drift observed today. When this drift reached a critical thickness for the environment, underlying ice would have been insulated from further ablation (Fitzsimons, 1990; Kowalewski et al., 2006). A process especially evident at the coastal valley mouths, where the deposit is characterised by well-preserved, buried glacial ice-cored moraine (e.g. Pollard et al., 2002; Levy et al., 2013).

An additional group of samples (LM3, 4 & 5) relate to the areal extent of Glacial Lake Trowbridge (see Clayton-Greene et al., 1988) and may provide some additional evidence concerning the lake's formation and decay within Miers Valley. We interpret the ridge like feature mapped at the margins of present day Lake Miers to be a product of a "lake-ice conveyor" process as described by Clayton-Greene et al. (1987); Hall et al., 2006; and Hendy et al., 2000, whereby englacial material is transported via lake ice towards its contemporary margins where it is re-deposited as ice rafted drift. Our mean exposure age of 21.8 ± 5.1 ka for the feature agrees with lacustrine sediments at Glacial Lake Washburn (Wright Valley, Stuiver et al., 1981) and at Glacial Lake Victoria (Victoria Valley, Hall et al., 2002) that indicate the presence of ice impounded pro-glacial lakes at 21 to 8.6 ka ^{14}C BP in the MDVs. Additionally, as the lacustrine radiocarbon ages from Glacial Lake Trowbridge (Clayton-Greene et al., 1988) span a similar range, 23 to 10 ka ^{14}C cal BP, it may suggest that a similar hydrological regime existed in the

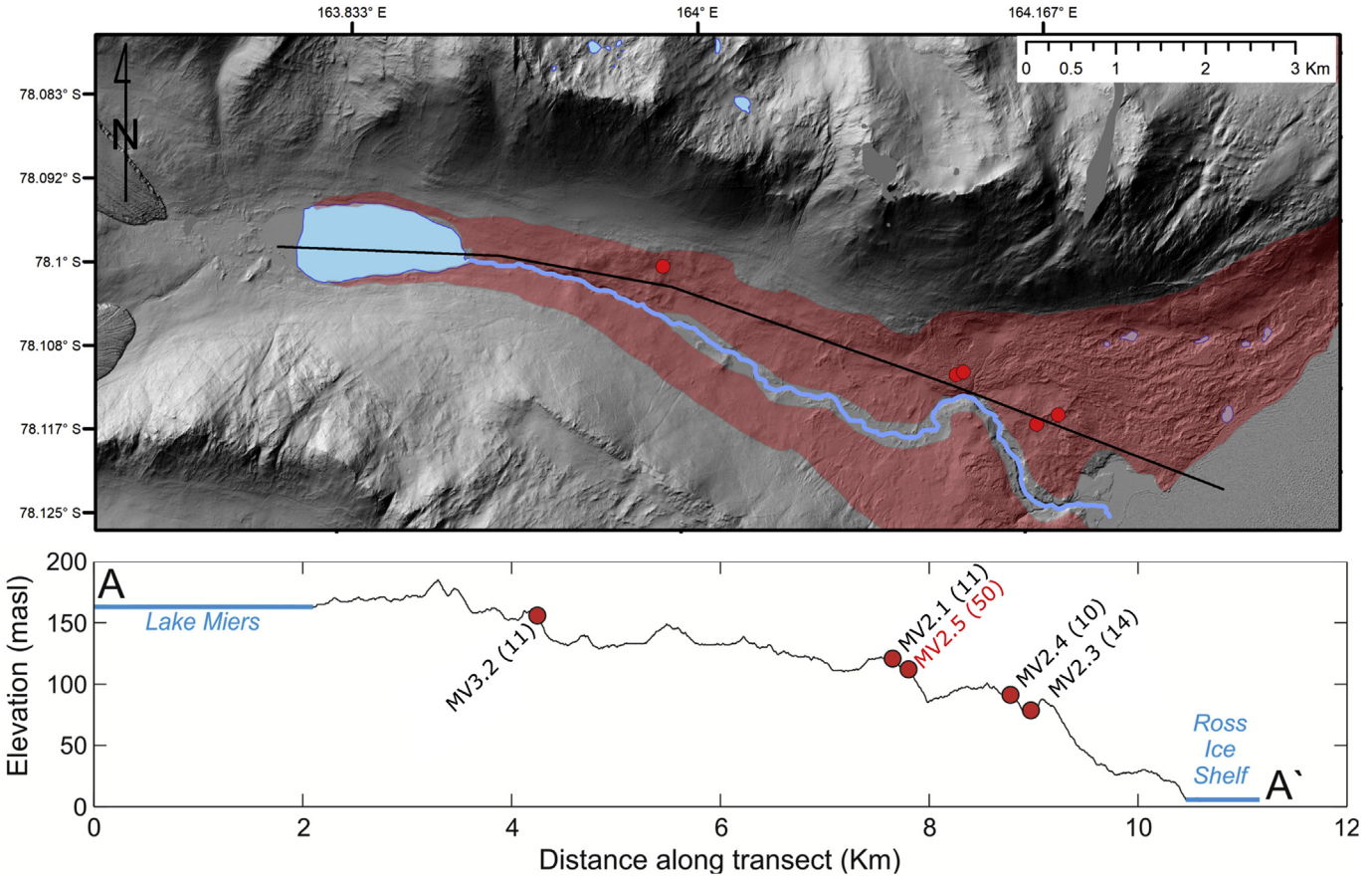

Fig. 6. Centreline profile of the Miers Valley running from Lake Miers (A) in the west to the Ross Ice Shelf (A') to the east (see Fig. 4 for regional setting). Location and bracketed age of SED samples collected from within the Ross Sea Drift (marked in red) along this transect estimate West Antarctic ice loss in the eastern section of the Miers Valley to be at least 120 m (see text). The direction of ice retreat/thinning is from left to right (A to A'). The position of sample MV2.5, assumed to be an outlier, is labelled in red. (For interpretation of the references to colour in this figure legend, the reader is referred to the web version of this article.)

Denton Hills. Although our exposure ages from the LM site appear to overlap the same period, they must be viewed with some caution. Ages of material exhumed at the glacier margin, transported and re-deposited via the "lake-ice conveyor", may reflect the combination of englacial inheritance, i.e. exposure during lake surface transport and deposition at its margin. In addition, as the time that material may have been covered by water at the lake margin is unknown, the effect on ^{10}Be production rate due to cosmic ray attenuation cannot be quantified. However, assuming the latter process is minimal we can conclude that over the past 22 ka at most, Lake Trowbridge was actively modifying the landscape.

5.1.2. Miers, Joyce and Garwood Glaciers

Exposure ages detailing the Late-Pleistocene behaviour of the three Denton Hills glaciers comprise the majority of our ^{10}Be dataset (n = 15) and range from 26 to 286 ka with a cluster of 13 ages from 26 to 51 ka.

Geomorphic field mapping and glacial evidence from terminal and lateral moraines associated with the Joyce, Adams and Miers glaciers show evidence of retreat from positions well beyond their current ice limits. Joyce Glacier appears to have advanced at least ~250 m eastward into Garwood Valley and the Adams-Miers glacier pair appears to have advanced ~1.2 km beyond its current extent.

At Garwood Glacier sample positions and age scatter infers that even with the omission of GG-8, the remaining age range of 26–51 ka is sufficiently large to restrict a detailed analysis of the timing of Garwood retreat which led to the deposition of the moraine complex. The morphology (e.g. Fig. 4D) shows two distinct moraine ridges however, GG4, the youngest sample, resides on the outer moraine about 50 m from the ice margin, and only tens of metres from the oldest sample, GG3. If the six samples for Garwood Glacier were treated as a single population with a mean value of 35.6 ka, our simplest conclusion would be that it has not advanced west into the Lake Colleen basin from its present terminal position for at least the past 26 ka and perhaps for as far back as 51 ka.

The Miers (31–44 ka), Joyce (33–36 ka) and Garwood glaciers (26–51 ka) appear to have all reached their maximum ice volumes prior to the global LGM (taken as 26–19 ka BP, Clark et al., 2009) and therefore, the colder climate during the peak and towards the end of the global LGM may have had little impact on the down valley extent of the local glacier systems and it appears most likely that these glaciers did not advance further than their present ice margins during the LGM.

5.2. Asynchronous deglaciations

Marchant et al. (1994), from observations of glacial sediments in the Taylor Valley, suggested that during interglacials, valley glaciers advanced while ice sheet margins thinned at coastal margins. In contrast, during glacial periods ice sheet margins thickened and valley glaciers retreated.

This investigation shows evidence of local glacial retreat both in and out of phase with global glacial cycles. The deposition and timing of RSD in Miers Valley by the RIS, displays a classic synchronous (or in-phase) response to climate. As global temperatures cooled prior to the LGM, advance of the RIS grounding line across the Ross Embayment followed by its retreat at the onset of warming after 20 ka, after the Last Interglacial, resulted in deposition of RSD. Conversely, the retreat of valley glaciers in the Denton Hills during global LGM times would appear to support the asynchronous (out of phase) deglaciation hypothesis.

We suggest that, since exposure ages reflect periods of glacial stagnation or ice retreat, local glaciers retreated prior to the local LGM. As the LGM Ross Embayment fully transitioned from an open ocean/ice shelf mosaic to an expansive grounded ice sheet, it would have both decreased evaporation rates and increased the distance to the nearest moisture source. This situation, combined with a cooler and drier climate during the LGM, implied by ice-core data (Jouzel et al., 2007; Petit et al., 1999), may have starved the local catchments of precipitation, thus prohibiting an advance and possibly triggering a period of retreat.

The Denton Hills valley glaciers display a somewhat asynchronous response to LGM cooling. These glaciers achieved their terminal positions marginally beyond or at their current ice limits during the period ~35–25 ka, but there is no record preserved of a major advance during the MIS-5 interglacial (~125 ka) at more distal locations such as that observed at the Darwin-Hatherton outlet glacier system (Fig. 1) in the Transantarctic Mountains (Joy et al., 2014). The only evidence of late to mid-Pleistocene glacial advances in the Denton Hills comes from the Miers Valley samples on slopes proximal to Miers lake (MG 6 and 7), with ages of 135 and 286 ka, respectively (given that MG8 and MG9 are outliers).

An explanation for the differences in the timing and magnitude of past glacier behaviour between sites at the Darwin-Hatherton and Denton Hills (~200 km) may be related to the geometry of the ice catchments that feed them. While the Darwin and Hatherton glaciers are directly connected, and may respond quickly to changes in EAIS ice volume, the Denton Hills glaciers are not. The presence and elevation (~3500 msl) of the Royal Society Range (Fig. 1) provides an effective barrier to ice flow into the region, thus isolating their glacial catchments from the influences of East Antarctic ice. The result of this topographic barrier is that the local catchments of various sizes may respond very differently, with the Garwood Glacier being fed by a small steep isolated alpine catchment (~12 km^2) and the Adams, Miers and Joyce glaciers fed by the much larger Blue Glacier catchment (~700 km^2).

5.3. Glacial history of the Denton Hills

Our field mapping and ^{10}Be exposure ages provide key insights into ice sheet and alpine glacier behaviour during the Late-Pleistocene in the Denton Hills. The development of the modern landscape within the Miers and Garwood valleys leads to a number of conclusions about the glacial dynamics and resulting processes from ~12 to 51 ka.

5.3.1. Pre-LGM

As the grounding line of the WAIS is thought to have been at its terminal position near the continental shelf well before the LGM (Denton and Hughes, 2000; Shipp and Domack, 1999; Stuiver et al., 1981) it is likely that the RIS intruded into the valley mouths by ~30 ka. The Miers and Adams glaciers may have coalesced and advanced into the Miers Valley forming the lateral moraine feature wrapping around the side of Holiday Peak and up valley from Lake Miers. At this time, supra-glacial meltwater generated during the cooler than present austral summer drained down valley and started forming Glacial Lake Trowbridge, whose exit was dammed against the intruded RIS margin.

Our two oldest dates from the Miers Valley (i.e. MG8 and MG9) and east of the modern Miers Glacier are ~166 ka and 245 ka, and much older. Because MIS 3 glacial deposits are rare (e.g. Swanger et al., 2017), these sites present important targets for future work.

During the same period, the Joyce Glacier expanded out to the northern flank of the Garwood Valley. Although the distribution of patterned ground observed on the valley wall, and which extends further past our sampled moraines, suggests that the Garwood and Joyce glaciers had coalesced in the past, it is likely that the maximum pre-LGM advance of the Joyce Glacier only reached the margin of Lake Colleen. The inference from the terminal positions of the two glaciers is that Lake Colleen had available space to

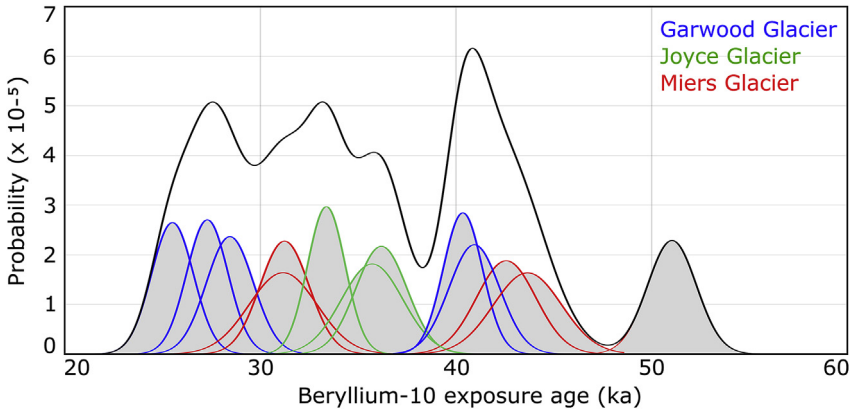

Fig. 7. Probability density plot (outliers excluded) for exposure ages from the Joyce (green, n = 3), Miers (red, n = 4) and Garwood (blue, n = 6) glaciers. Plots are calculated as per Lowell (1995) and use the internal (analytical) age error (see Table 2). (For interpretation of the references to colour in this figure legend, the reader is referred to the web version of this article.)

occupy the basin for at least the last ~51 ka.

5.3.2. LGM to present

The behaviour of the Denton Hills valley glaciers during the LGM is not well defined. Fig. 7 shows the cumulative age probability plot (Lowell, 1995) for all 13 ages in the range from 26 to 51 ka from the Denton Hills with a population mean of 35.9 ± 7.5 ka (1σ). The absence of glacial landforms with a majority of exposure ages commensurate with an Antarctic (or local) LGM at 18–22 ka, as defined by the onset of warming evidenced in numerous Antarctic ice cores (Augustin et al., 2004; Petit et al., 1999) indicates that the local LGM in the Denton Hills preceded the global LGM. Hence, we conclude the last advance of the Denton Hills glaciers most likely occurred prior to the global LGM sometime between ~26 and ~44 ka. Our exposure ages cannot preclude the occurrence of an advance at the global LGM or even during the current interglacial if evidence for that advance was removed or is obscured. The only two possibilities are that any advance younger than ~20 ka was removed by the incursion of an expanding RIS or, that advance now abuts the pre-LGM moraines we have dated. We believe both options re highly improbable and hence conclude that the modern terminal moraines represent the local LGM.

Clayton-Greene et al. (1988) suggest that Glacial Lake Trowbridge was at its maximum extent at the local LGM with a maximum elevation just above that of modern Lake Miers and had started to drain prior to 14 ka, likely driven by the thinning of the detached ice in the valley mouths. The youngest Lake Miers site age of 16.5 ka (LM4) would thus support this observation and conclude that the lake had considerably reduced in volume. The inference from this is that a considerable proportion of the lake volume was lost, likely via evaporation, before ~14 ka.

Falling lake levels in the Holocene appear to have coincided with the continued thinning of the RIS. This process continued until ~9 ka when valley mouths became predominantly ice-free, the eastern basin in the Miers Valley now being drained and in-filled with glacio-lacustrine and evaporite sediments, while the western basin still contained water and formed the modern Lake Miers.

As the remaining stranded ice in the valley mouth sublimated, englacial material slowly accumulated and was deposited throughout the valley floors as the Ross Sea Drift. The RSD was further modified by fluvial and aeolian reworking of the post-glacial landscape. In both Miers and Garwood valleys, periods of enhanced meltwater generation from the alpine glaciers, transported sandy material down valley to produce large deltas. Meltwater streams and rivers have continued to incise and rework sediments, particularly in ice-cored moraines, in the glacial outwash plains and valley floor drainage channels.

6. Conclusions

Surface exposure ages from a variety of glacial and lacustrine features in the Garwood and Miers valleys of the Denton Hills provide new insights into the behaviour of small alpine-style polar glaciers as well as those of the Ross Ice Shelf over the last ~51 ka. Within the Denton Hills our 22 new exposure ages (omitting four outliers) range from 10 to 286 ka and show that:

- Exposure ages representing the local LGM in the Denton Hills range from 26 to 51 ka with a preferred mean age of 35.9 ± 7.5 (1σ) based on 13 boulders taken from the terminal moraines of the Garwood, Joyce and Miers glaciers.
- The dated terminal moraines are either adjacent to today's modern ice margin or at most 100 m down valley from the current ice limits, suggesting that no younger advance has occurred beyond these limits since their deposition at 36 ka.
- The Lake Colleen basin, in the Garwood Valley, has been glacier-free since at least 26 ka.
- Glacial Lake Trowbridge over the past 23 ka at most, was actively modifying the landscape surrounding both the western and eastern basins.
- The Ross Sea Drift was deposited in the valley mouths when West Antarctic ice thinned at ~12–14 ka. The small age range from our exposure ages suggests an overall rapid thinning of ice, with most areas exposed at the same time.
- The lack of a significant regional expansion of valley glaciers in the Denton Hills during global LGM times appears to support the Marchant et al. (1994) asynchronous (out of phase) deglaciation hypothesis.

Acknowledgements

This research was supported by Antarctica New Zealand (for logistics) and the Australian Institute of Nuclear Science of Engineering for AMS measurements (AINGRA 09066). We thank: Rob Spiers, Sacha Baldwin-Cunningham and James Oram at the University of Canterbury cosmogenic preparation lab; Mike Bentley at Durham University for sample collection and Charles Mifsud at ANSTO for AMS preparation. KJ is supported by a NZ Ministry of

Business and Innovation environment research grant (UOWX1401). GDP is supported by the Universidad de Chile Academic start-up fund and Chilean Fondecyt grant number 11160038.

Appendix A. Supplementary data

Supplementary data related to this article can be found at https://doi.org/10.1016/j.quascirev.2017.11.002.

References

Ackert, R.P., Kurz, M.D.T., 2004. Age and uplift rates of Sirius Group sediments in the Dominion Range, Antarctica, from surface exposure dating and geomorphology. Glob. Planet. Change 42, 207–225. https://doi.org/10.1016/j.gloplacha.2004.02.001.

Ackert, R.P., Mukhopadhyay, S., Parizek, R., Borns, H.W., 2007. Ice elevation near the west Antarctic ice sheet divide during the last glaciation. Geophys. Res. Lett. 34, L21506 https://doi.org/10.1029/2007GL031412.

Ackert, R.P., Putnam, A.E., Mukhopadhyay, S., Pollard, D., DeConto, R.M., Kurz, M.D.T., Borns, H.W., 2013. Controls on interior West Antarctic Ice Sheet Elevations: inferences from geologic constraints and ice sheet modeling. J. Quat. Sci. 65, 26–38. https://doi.org/10.1016/j.quascirev.2012.12.017.

Anderson, J.B., Conway, H., Bart, P.J., Witus, A.E., Greenwood, S.L., McKay, R.M., Hall, B.L., Ackert, R.P., Licht, K., Jakobsson, M., Stone, J.O., 2014. Ross Sea paleo-ice sheet drainage and deglacial history during and since the LGM. Quat. Sci. Rev. 100, 31–54. https://doi.org/10.1016/j.quascirev.2013.08.020.

Applegate, P.J., Urban, N.M., Laabs, B.J.C., Keller, K., Alley, R.B., 2010. Modeling the statistical distributions of cosmogenic exposure dates from moraines. Geosci. Model Dev. 3, 293–307. https://doi.org/10.5194/gmd-3-293-2010.

Atkins, C.B., 2013. Geomorphological evidence of cold-based glacier activity in South Victoria Land, Antarctica. Geol. Soc. Lond. Spec. Publ. 381.

Augustin, L., et al., 2004. Eight glacial cycles from an Antarctic ice core. Nature 429, 623–628.

Balco, G., 2011. Contributions and unrealized potential contributions of cosmogenic-nuclide exposure dating to glacier chronology, 1990–2010. J. Quat. Sci. 30 (1–2), 3–27. https://doi.org/10.1016/j.quascirev.2010.11.003.

Balco, G., Stone, J.O., Lifton, N.A., Dunai, T.J., 2008. A complete and easily accessible means of calculating surface exposure ages or erosion rates from 10Be and 26Al measurements. Quat. Geochronol. 3, 174–195. https://doi.org/10.1016/j.quageo.2007.12.001.

Reconstruction of Antarctic ice sheet deglaciation (RAISED). In: Bentley, M.J., O Cofaigh, C., Anderson, J.B. (Eds.), Quat. Sci. Rev. 100, 1–158.

Brook, E.J., Brown, E.T., Kurz, M.D.T., Ackert, R.P., Raisbeck, G.M., Yiou, F., 1995a. Constraints on age, erosion, and uplift of Neogene glacial deposits in the Transantarctic Mountains determined from in situ cosmogenic 10Be and 26Al. Geology 23, 1063–1066. https://doi.org/10.1130/0091-7613(1995)023<1063.

Brook, E.J., Kurz, M.D.T., Ackert, R.P., 1993. Chronology of Taylor glacier advances in Arena valley, Antarctica, using in situ cosmogenic 3He and 10Be. Quat. Res. 39, 11–23.

Brook, E.J., Kurz, M.D.T., Ackert, R.P., Raisbeck, G.M., Yiou, F., 1995b. Cosmogenic nuclide exposure ages and glacial history of late-Quaternary Ross Sea drift in McMurdo Sound, Antarctica. Earth Planet. Sci. Lett. 131, 41–56. https://doi.org/10.1016/0012-821X (95)00006-X.

Brown, E.T., Edmond, J.M., Raisbeck, G.M., Yiou, F., Kurz, M.D.T., Brook, E.J., 1991. Examination of surface exposure ages of Antarctic moraines using in situ produced 10Be and 26Al. Geochim. Cosmochim. Acta 55, 2269–2283.

Child, D., Elliott, G., Mifsud, C., Smith, A.M., Fink, D., 2000. Sample processing for earth science studies at ANTARES. Nucl. Instrum. Methods Phys. Res. Sect. A Accel. Spectrom. Detect. Assoc. Equip. 172, 856–860. https://doi.org/10.1016/S0168-583X (00)00198-1.

Clark, P.U., Dyke, A.S., Shakun, J.D., Carlson, A.E., Clark, J., Wohlfarth, B., Mitrovica, J.X., Hostetler, S., McCabe, A.M., 2009. The last glacial maximum. Sci. (80) 325, 710–714. https://doi.org/10.1126/science.1172873.

Clayton-Greene, J.M., Hendy, C.H., Denton, G.H., 1987. The origin of drift mounds in Miers Valley, Antarctica. Antarct. J. U. S. 59–61.

Clayton-Greene, J.M., Hendy, C.H., Hogg, A.G., 1988. Chronology of a Wisconsin age proglacial lake in the Miers valley, Antarctica. New Zeal. J. Geol. Geophys. 31, 353–361. https://doi.org/10.1080/00288306.1988.10417781.

Conway, H., Hall, B.L., Denton, G.H., Gades, A.M., Waddington, E.D., 1999. Past and future grounding-line retreat of the west Antarctic ice sheet. Sci. (80) 286, 280–283. https://doi.org/10.1126/science.286.5438.280.

Cox, S., Turnbull, I.M., Issac, M.J., Townsend, D.B., Smith-Lyttle, B., 2012. Geology of Southern Victoria Land, Antarctica. Lower Hutt, New Zealand.

Denton, G.H., Hughes, T.J., 2000. Reconstruction of the Ross Ice Drainage System, Antarctica, at the last glacial maximum. Geogr. Ann. Phys. Geogr. 82 (2–3), 143–166. https://doi.org/10.1111/j.0435-3676.2000.00120.x.

Denton, G.H., Marchant, D.R., 2000. The geologic basis for a reconstruction of a grounded ice sheet in McMurdo Sound, Antarctica, at the Last Glacial Maximum. Geogr. Ann. Ser. A Phys. Geogr. 82, 167–211.

Desilets, D., Zreda, M.G., Prabu, T., 2006. Extended scaling factors for in situ cosmogenic nuclides: new measurements at low latitudes. Earth Planet. Sci. Lett. Elsevier 246 (3), 265–276.

Dunai, T.J., 2000. Scaling factors for production rates of in situ produced cosmogenic nuclides: a critical reevaluation. Earth Planet. Sci. Lett. Elsevier 176 (1), 157–169.

Fink, D., Smith, A.M., 2007. An inter-comparison of 10Be and 26Al AMS reference standards and the 10Be half-life. Nucl. Instrum. Methods Phys. Res. Sect. B Beam Interact. Mater. Atoms 259, 600–609. https://doi.org/10.1016/j.nimb.2007.01.299.

Fitzsimons, S.J., 1990. Ice-marginal depositional processes in a polar maritime environment, Vestfold Hills, Antarctica. J. Glaciol. 36 (124), 279–286. https://doi.org/10.3189/002214390793701255.

Greenwood, S.L., Gyllencreutz, R., Jakobsson, M., Anderson, J.B., 2012. Ice-flow switching and east/West Antarctic ice sheet roles in glaciation of the western Ross sea. Geol. Soc. Am. Bull. 124, 1736–1749. https://doi.org/10.1130/B30643.1.

Hall, B.L., Denton, G.H., 2000. Radiocarbon chronology of Ross sea drift, eastern Taylor Valley, Antarctica: evidence for a grounded ice sheet in the Ross sea at the last glacial maximum. Geogr. Ann. Ser. A Phys. Geogr. 82, 305–336.

Hall, B.L., Denton, G.H., Overturf, B., Hendy, C.H., 2002. Glacial Lake Victoria, a high-level Antarctic lake inferred from lacustrine deposits in Victoria valley. J. Quat. Sci. 17, 697–706. https://doi.org/10.1002/jqs.691.

Hall, B.L., Denton, G.H., Stone, J.O., Conway, H., 2013. History of the grounded ice sheet in the Ross Sea sector of Antarctica during the Last Glacial Maximum and the last termination. Geol. Soc. Lond. Spec. Publ. 381 https://doi.org/10.1144/SP381.5.

Hall, B.L., Hendy, C.H., Denton, G.H., 2006. Lake-ice conveyor deposits: geomorphology, sedimentology, and importance in reconstructing the glacial history of the Dry valleys. Geomorphology 75, 143–156. https://doi.org/10.1016/j.geomorph.2004.11.025.

Hawke, R.M., McConchie, J.A., 2001. Bedload transport in a meltwater stream, Miers Valley, Antarctica: controls and prediction. J. Hydrol. 40, 1–18.

Hein, A.S., Fogwill, C.J., Sugden, D.E., Xu, S., 2011. Glacial/interglacial ice-stream stability in the Weddell Sea embayment, Antarctica. Earth Planet. Sci. Lett. 307 (1), 211–221. Available at: http://www.sciencedirect.com/science/article/pii/S0012821X11002536. (Accessed 22 October 2013).

Hendy, C.H., Sadler, A.J., Denton, G.H., Hall, B.L., 2000. Proglacial lake-ice conveyors: a new mechanism for deposition of drift in polar environments. Geogr. Ann. Ser. A Phys. Geogr. 82, 249–270. https://doi.org/10.1111/j.0435-3676.2000. 00124.x.

Heyman, J., Applegate, P.J., Blomdin, R., Gribenski, N., Harbor, J.M., Stroeven, A.P., 2016. Boulder height - exposure age relationships from a global glacial 10Be compilation. Quat. Geochronol. Elsevier B.V 34, 1–11. https://doi.org/10.1016/j.quageo.2016.03.002.

Higgins, S.M., Hendy, C.H., Denton, G.H., 2000. Geochronology of Bonney drift, Taylor Valley, Antarctica: evidence for interglacial expansions of Taylor glacier. Geogr. Ann. Ser. A Phys. Geogr. 82A (2&3), 391–409. https://doi.org/10.1111/1468-0459.00130.

Jouzel, J., Masson-Delmotte, V., Cattani, O., Dreyfus, G., Falourd, S., Hoffmann, G., Minster, B., Nouet, J., Barnola, J.M., Chappellaz, J., Fischer, H., Gallet, J.C., Johnsen, S.J., Leuenberger, M., Loulergue, L., Luethi, D., Oerter, H., Parrenin, F., Raisbeck, G.M., Raynaud, D., Schilt, A., Schwander, J., Selmo, E., Souchez, R., Spahni, R., Stauffer, B., Steffensen, J.P., Stenni, B., Stocker, T.F., Tison, J.L., Werner, M., Wolff, E.W., 2007. Orbital and millennial Antarctic climate variability over the past 800,000 years. Sci. (80) 317, 793–796. https://doi.org/10.1126/science.1141038.

Joy, K., Fink, D., Storey, B.C., Atkins, C.B., 2014. A 2-million-year glacial chronology of the Hatherton glacier, Antarctica and implications for the size of the east Antarctic ice sheet at the last glacial maximum. J. Quat. Sci. 83, 46–57.

Kaplan, M.R., Licht, K.J., Winckler, G., Schaefer, J.M., Bader, N., Mathieson, C., Roberts, M., Kassab, C.M., Schwartz, R., Graly, J.A., 2017. Middle to late Pleistocene stability of the central East Antarctic ice sheet at the head of Law glacier. Geology. https://doi.org/10.1130/G39189.1.

Korschinek, G., Bergmaier, A., Faestermann, T., Gerstmann, U.C., Knie, K., Rugel, G., Wallner, A., Dillmann, I., Dollinger, G., von Gostomski, C.L., 2010. A new value for the half-life of 10Be by Heavy-ion elastic recoil detection and liquid scintillation counting. Nucl. Instrum. Methods Phys. Res. Sect. B Beam Interact. Mater. Atoms. Elsevier B.V. 268 (2), 187–191. https://doi.org/10.1016/j.nimb.2009.09.020.

Kowalewski, D.E., Marchant, D.R., Levy, J.S., Head, J.W., 2006. Quantifying low rates of summertime sublimation for buried glacier ice in Beacon Valley, Antarctica. Antarct. Sci. 18, 421–428. https://doi.org/10.1017/S0954102006000460.

Larter, R.D., Anderson, J.B., Graham, A.G.C., Gohl, K., Hillenbrand, C.D., Jakobsson, M., Johnson, J.S., Kuhn, G., Nitsche, F.O., Smith, J.A., Witus, A.E., Bentley, M.J., Dowdeswell, J.A., Ehrmann, W., Klages, J.P., Lindow, J., Cofaigh, C.Ó., Spiegel, C., 2014. Reconstruction of changes in the Amundsen sea and Bellingshausen sea sector of the west Antarctic ice sheet since the last glacial maximum. Quat. Sci. Rev. 100, 55–86. https://doi.org/10.1016/j.quascirev.2013.10.016.

Levy, J.S., Fountain, A.G., O'Connor, J.E., Welch, K.A., Lyons, W.B., 2013. Garwood valley, Antarctica: a new record of last glacial maximum to Holocene glaciofluvial processes in the McMurdo dry valleys. Geol. Soc. Am. Bull. 125, 1484–1502. https://doi.org/10.1130/B30783.1.

Lifton, N.A., Smart, D.F., Shea, M.A., 2008. Scaling time-integrated in situ cosmogenic nuclide production rates using a continuous geomagnetic model. Earth Planet. Sci. Lett. Elsevier 268 (1), 190–201.

Lilly, K., Fink, D., Fabel, D., Lambeck, K., 2010. Pleistocene dynamics of the interior East Antarctic ice sheet. Geology 38, 703–706. https://doi.org/10.1130/G31172x.1.

Lowell, T.V., 1995. The application of radiocarbon age estimates to the dating of glacial sequences: an example from the Miami sublobe, Ohio, U.S.A. J. Quat. Sci. 14, 85–99. https://doi.org/10.1016/0277-3791(94)00113-P.

Mackintosh, A., Verleyen, E., O'Brien, P.E., White, D.A., Jones, R.S., McKay, R., Dunbar, R., Gore, D.B., Fink, D., Post, A.L., Miura, H., Leventer, A., Goodwin, I., Hodgson, D.A., Lilly, K., Crosta, X., Golledge, N.R., Wagner, B., Berg, S., van Ommen, T., Zwartz, D., Roberts, S.J., Vyverman, W., Masse, G., 2014. Retreat history of the east Antarctic ice sheet since the last glacial maximum. Quat. Sci. Rev. 100, 10–30. https://doi.org/10.1016/j.quascirev.2013.07.024.

Mackintosh, A., White, D.A., Fink, D., Gore, D.B., Pickard, J., Fanning, P.C., 2007. Exposure ages from East Antarctic ice sheet since the last glacial maximum. Quat. Sci. Rev. Doi: mountain dipsticks in mac. Robertson land, east Antarctica, indicate little change in ice-sheet thickness since the last glacial maximum. Geology 35, 551–554. https://doi.org/10.1130/G23503A.1.

Marchant, D.R., Denton, G.H., Bockheim, J.G., Wilson, S.C., Kerr, A.R., 1994. Quaternary changes in level of the upper Taylor glacier, Antarctica: implications for paleoclimate and east Antarctic ice sheet dynamics. Boreas 23, 29–43.

McConchie, J.A., 1989. The hydrology, glaciology and sediment transport processes of the Miers Valley (K046) Title. New Zeal. Antarct. Rec. 9, 17–18.

McKay, R., Golledge, N.R., Maas, S., Naish, T., Levy, R., Dunbar, G., Kuhn, G., 2016. Antarctic marine ice-sheet retreat in the Ross Sea during the early Holocene. Geology 44, 7–10. https://doi.org/10.1130/G37315.1.

McKay, R.M., Dunbar, G.B., Naish, T.R., Barrett, P.J., Carter, L., Harper, M., 2008. Retreat history of the Ross ice sheet (shelf) since the last glacial maximum from deep-basin sediment cores around Ross Island. Palaeogeogr. Palaeoclimatol. Palaeoecol. 260, 245–261. https://doi.org/10.1016/j.palaeo.2007.08.015.

McKay, R.M., Naish, T.R., Powell, R.D., Barrett, P.J., Scherer, R.P., Talarico, F., Kyle, P., Monien, D., Kuhn, G., Jackolski, C., Williams, T., 2012. Pleistocene variability of Antarctic ice sheet extent in the Ross embayment. J. Quat. Sci. 34, 91–112. https://doi.org/10.1016/j.quascirev.2011.12.012.

Mifsud, C., Fujioka, T., Fink, D., 2012. Extraction and purification of quartz in rock using hot phosphoric acid for in situ cosmogenic exposure dating. Nucl. Instrum. Methods Phys. Res. Sect. B Beam Interact. Mater. Atoms 294, 203–207. https://doi.org/10.1016/j.nimb.2012.08.037.

Morgan, D.J., Putkonen, J., Balco, G., Stone, J.O., 2011. Degradation of glacial deposits quantified with cosmogenic nuclides, Quartermain Mountains, Antarctica. Earth Surf. Process. Landforms 36, 217–228. https://doi.org/10.1002/esp.2039.

Mukhopadhyay, S., Ackert, R.P., Pope, A.E., Pollard, D., DeConto, R.M., 2012. Miocene to recent ice elevation variations from the interior of the West Antarctic Ice Sheet: constraints from geologic observations, cosmogenic nuclides and ice sheet modeling. Earth Planet. Sci. Lett. 337–338, 243–251. https://doi.org/10.1016/j.epsl.2012.05.015.

Nishiizumi, K., Imamura, M., Caffee, M.W., Southon, J.R., Finkel, R.C., Mcaninch, J., 2007. Absolute calibration of 10Be AMS standards. Nucl. Instrum. Methods Phys. Res. Sect. B Beam Interact. Mater. Atoms 258 (2), 403–413. https://doi.org/10.1016/j.nimb.2007.01.297.

Ó Cofaigh, C., Davies, B.J., Livingstone, S.J., Smith, J.A., Johnson, J.S., Hocking, E.P., Hodgson, D.A., Anderson, J.B., Bentley, M.J., Canals, M., Domack, E., Dowdeswell, J.A., Evans, J., Glasser, N.F., Hillenbrand, C.D., Larter, R.D., Roberts, S.J., Simms, A.R., 2014. Reconstruction of ice-sheet changes in the Antarctic Peninsula since the last glacial maximum. Quat. Sci. Rev. 100, 87–110. https://doi.org/10.1016/j.quascirev.2014.06.023.

Petit, J.R., Jouzel, J., Raynaud, D., Barkov, N.I., Barnola, J.M., Basile, I., Bender, M., Chappellaz, J., Davisk, M., Delaygue, G., Delmotte, M., Kotlyakov, V.M., Legrand, M., Lipenkov, V.Y., Lorius, C., Pepin, L., Ritz, C., Saltzmank, E., Stievenard, M., 1999. Climate and atmospheric history of the past 420,000 years from the Vostok ice core, Antarctica. Nature 399, 429–436.

Pollard, W., Doran, P., Wharton, R., 2002. The nature and significance of massive ground ice in Ross sea drift, Garwood valley, McMurdo sound. R. Soc. N. Z. Bull. 35, 397–404.

Putkonen, J., Connolly, J., Orloff, T., 2008. Landscape evolution degrades the geologic signature of past glaciations. Geomorphology 97, 208–217. https://doi.org/10.1016/j.geomorph.2007.02.043.

Shipp, S., Domack, E.W., 1999. Late Pleistocene - Holocene retreat of the west Antarctic ice sheet system in the Ross sea: Part 1 — geophysical results. Geol. Soc. Am. Bull. 111, 1517–1536.

Spigel, R., Priscu, J.C., 1998. Physical Limnology of the McMurdo Dry Valleys Lakes. American Geophysical Union.

Stone, J.O., Balco, G., Sugden, D.E., Caffee, M.W., Sass, L.C., Cowdery, S., Siddoway, C., 2003. Holocene deglaciation of marie Byrd land, west Antarctica. Sci. (80) 299, 99–102. https://doi.org/10.1126/science.1077998.

Storey, B.C., Fink, D., Hood, D., Joy, K., Shulmeister, J., Riger-Kusk, M., Stevens, M.I., 2010. Cosmogenic nuclide exposure age constraints on the glacial history of the Lake Wellman area, Darwin Mountains, Antarctica. Antarct. Sci. 22, 603–618. https://doi.org/10.1017/S0954102010000799.

Strasky, S., Di Nicola, L., Baroni, C., Salvatore, M.C., Baur, H., Kubik, P.W., Schlüchter, C., Wieler, R., 2009. Surface exposure ages imply multiple low-amplitude Pleistocene variations in East Antarctic Ice Sheet, Ricker Hills, Victoria Land. Antarct. Sci. 21 (1), 59–69. https://doi.org/10.1017/S0954102008001478.

Stuiver, M., Denton, G.H., Hughes, T.J., Fastook, J.L., 1981. History of the marine ice sheet in West Antarctica during the last glaciation: a working hypothesis. In: Denton, G.H., Hughes, T. (Eds.), The Last Great Ice Sheets. Wiley, New York, pp. 319–436.

Suganuma, Y., Miura, H., Zondervan, A., Okuno, J., 2014. East Antarctic deglaciation and the link to global cooling during the Quaternary: evidence from glacial geomorphology and 10Be surface exposure dating of the Sør Rondane Mountains, Dronning Maud Land. Quat. Sci. Rev. Elsevier Ltd 97, 102–120. https://doi.org/10.1016/j.quascirev.2014.05.007.

Sugden, D.E., Denton, G.H., Marchant, R., 1995. Evolution of the dry valleys, trans-antarctic mountains: tectonic implications. J. Geophys. Res. - Earth Surf. 100, 9949–9967.

Sugden, D.E., Summerfield, M.A., Denton, G.H., Wilch, T.I., McIntosh, W.C., Marchant, D.R., Rutford, R.H., 1999. Landscape development in the royal society range, southern Victoria land, Antarctica: stability since the mid-miocene. Geomorphology 28, 181–200.

Swanger, K.M., Lamp, J.L., Winckler, G., Schaefer, J.M., Marchant, D.R., 2017. Glacier advance during marine Isotope stage 11 in the McMurdo dry valleys of Antarctica. Sci. Rep. 7, 41433.

White, D.A., Fülöp, R.H., Bishop, P., Mackintosh, A., Cook, G., 2011. Can in-situ cosmogenic 14C be used to assess the influence of clast recycling on exposure dating of ice retreat in Antarctica? Quat. Geochronol. 6, 289–294. https://doi.org/10.1016/j.quageo.2011.03.004.

Yamane, M., Yokoyama, Y., Miura, H., Maemoku, H., Iwasaki, S., Matsuzaki, H., 2011. The last deglacial history of Lützow-Holm Bay, East Antarctica. J. Quat. Sci. 26, 3–6. https://doi.org/10.1002/jqs.1465.

Zachos, J., Pagani, M., Sloan, L., Thomas, E., Billups, K., 2001. Trends, rhythms, and aberrations in global climate 65 Ma to present. Science 292 (5517), 686–693. https://doi.org/10.1126/science.1059412.